

BEST ANISOTROPIC 3-D WAVELET DECOMPOSITION IN A RATE-DISTORTION SENSE

Emmanuel Christophe[†], Corinne Mailhes[†] and Pierre Duhamel^{}*

[†] TésA/IRIT, 14-16 port St Etienne, 31000 Toulouse, France

^{*} CNRS/LSS, Supelec Plateau de moulon, F-91192 Gif-sur-Yvette Cedex, France

e.christophe@ieee.org, corinne.mailhes@enseeiht.fr, pierre.duhamel@lss.supelec.fr

ABSTRACT

Hyperspectral sensors have been of a growing interest over the past few decades for Earth observation as well as deep space exploration. However, the amount of data provided by such sensors requires an efficient compression system which is yet to be defined. It is hoped that the particular statistical properties of such images can be used to obtain very efficient compression algorithms.

This paper proposes a method to find the most suitable wavelet decomposition for hyperspectral images and introduces the possibility of non isotropic decomposition. The decomposition is made by choosing the decomposition that provides an optimal rate-distortion trade-off. The obtained decomposition exhibits better performances in terms of rate-distortion curves compared to isotropic decomposition for high bitrates as well as for low bitrates.

1. INTRODUCTION

Earth observation from space has been of a growing interest since the first launch of an observation satellite a few decades ago. Deep space missions for the observation of the sun, planets, or comets have also become more common and share the same concerns.

As these missions seek better data quality to improve the scientific value of the information provided, performances of sensors improve with an increase in the spatial resolution, the radiometric precision, and possibly the number of spectral bands. Hyperspectral sensors provide valuable information about the observed object. Hyperspectral imagery, or spectral imagery, consists in observing the same scene at different wavelengths.

Typically, each image pixel is represented by hundreds of values, corresponding to various wavelengths. These values correspond to a sampling of the continuous spectrum emitted by the pixel. This high resolution spectrum sampling allows pixel identification (materials, mineral and gases...). The availability of the spectral information for each pixel leads to new applications in all fields that use remote sensing data (agriculture, environment, or military), and can help to improve the understanding of the solar system.

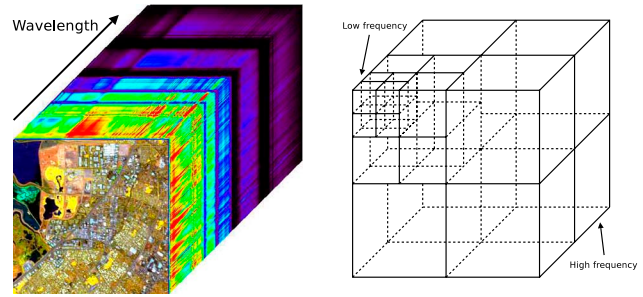


Fig. 1. Hyperspectral data cube and an example of isotropic wavelet decomposition.

However, hyperspectral sensors produce a considerable amount of information. Data transmission bandwidth and on-board storage capabilities are already limited for earth observation satellites, but constraints are even tighter for deep space missions. Therefore, the compression step becomes a crucial part of the acquisition system to enhance the ability to store, access and transmit information.

The specific redundancy between the different wavelength bands makes hyperspectral data an ideal candidate for compression. However, a suitable and adapted compression system is still being awaited. As an example, the spaceborne hyperspectral instrument Hyperion on EO-1 does not use compression, thus limiting the amount of data provided.

Existing works focus mainly on two different techniques, namely vector quantization and wavelets. A wavelet-based compression system based on SPIHT technique has been used successfully for the deep space probe Rosetta and for the Cassini mission [1]. Other adaptations of the successful wavelet-based SPIHT technique from Pearlman seem to be promising [2].

Most current hyperspectral wavelet compression algorithms are based on an isotropic decomposition of the hyperspectral data cube (Fig. 1) and, as a consequence, the spectral dimension is processed in the same manner as the spatial dimensions. Since the dimensions possess different properties [3], this is clearly not the optimal way to proceed.

For natural images, Ramchandran and Vetterli in [4] define a method to find the best wavelet decomposition and

quantization for a specific 2D-image. Their technique leads to a decomposition of the image based on a quadtree structure and only consider square subbands. In the natural image case, this regular structure is not a real problem since an image has similar properties along the vertical and the horizontal directions.

A search for non-isotropic decompositions for natural 2D images has been made by Xu and Do in [5] and shows that non-isotropic decompositions give better performances than isotropic decompositions in some cases for natural images. However, the search was not defined within the context of rate-distortion optimisation and some conditions on the search limited the generalization. If the results obtained by non-isotropic decomposition are better for natural images, the improvement for hyperspectral images, which are highly non-isotropic, can be expected to be greater.

This paper defines the theoretical structure for 3D non isotropic decompositions in section 2 and adapts the work of Ramchandran and Vetterli to find the most suitable decomposition for hyperspectral images in section 3. The decomposition is made by choosing the optimal rate-distortion trade-off, according to the possibilities of decomposition. These results are presented in section 4. Perspectives of future evolution are described in section 5.

2. ANISOTROPIC DECOMPOSITION

Traditionally, on 2-D images, the wavelet decomposition is isotropic i.e. for one given subband, the level of decomposition in the horizontal direction is the same as the level of decomposition in the vertical direction. This alternation between horizontal and vertical decompositions leads to square subbands (cubes, in the case of 3D data). This is the case for the multiresolution decomposition of Mallat [6] or the wavelet packets decomposition. This process is justified by the properties of traditional images: their statistical properties are quite similar in all directions.

Thus, we denote $W_{i,j,k}^{p,q,r}$ the wavelet subband space (Fig. 2):

- i, j, k corresponding to the row level, column level and spectral level respectively (implying the dimension of the considered subband).
- p, q, r being the row, column and spectral indexes respectively.

A relation can be defined between subbands. For a row decomposition, the anisotropic wavelet space satisfies

$$W_{i,j,k}^{p,q,r} = W_{i+1,j,k}^{2p,q,r} \oplus W_{i+1,j,k}^{2p+1,q,r}. \quad (1)$$

For a column decomposition,

$$W_{i,j,k}^{p,q,r} = W_{i,j+1,k}^{p,2q,r} \oplus W_{i,j+1,k}^{p,2q+1,r}. \quad (2)$$

And for a spectral decomposition,

$$W_{i,j,k}^{p,q,r} = W_{i,j,k+1}^{p,q,2r} \oplus W_{i,j,k+1}^{p,q,2r+1}. \quad (3)$$

For any step of the decomposition, for all subbands, we are able to choose the direction of the next decomposition, thus increasing the flexibility of the space decomposition. Both multiresolution decomposition and wavelet packet decomposition are special cases of this representation. The isotropic 3D structure considered in [2] as well as the *2D spatial+1D spectral* decomposition used in [7] for video coding are considered within this general framework.

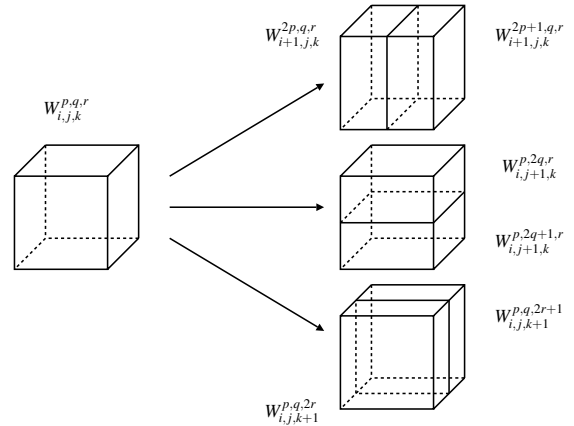


Fig. 2. Anisotropic decomposition and notations.

3. RATE-DISTORTION OPTIMIZATION

3.1. The allocation problem

The problem of bit allocation, i.e. distributing optimally the given bit budget between the subbands, is a classical problem in data compression. Shoham and Gersho [8] address this problem within the framework of rate-distortion theory. Their solution consists in minimizing the distortion under the constraint of the available bit budget.

Within the context of wavelet decomposition, different quantizers can be used for different subbands. Let S be the finite set of the quantizer combination for the subbands, let B be one element of S . The problem is to minimize the total distortion $D(B)$ for the given combination of quantizers, B , with the total rate $R(B)$ within the bit budget R_c :

$$\min_{B \in S} \{D(B)\} \text{ under } R(B) \leq R_c. \quad (4)$$

Using the Lagrangian method, this minimization under constraint becomes the minimization of the Lagrangian cost function J without constraint:

$$J(\lambda) = D + \lambda R. \quad (5)$$

In the context of independent coded subbands, using additive measures for rate and distortion, it can be shown that R-D

optimality is attained when *all subbands* operate at a constant slope point λ on their R-D curve. Thus, the problem becomes

$$\min \{D_k + \lambda R_k\} \text{ for each subband } k. \quad (6)$$

3.2. Algorithm

The algorithm is defined to search the best decomposition simultaneously with the best operating point. For one given subband, the algorithm computes the R-D points for different quantizers, thus leading to the R-D curve for the current subband. The R-D curve is also computed for the 3 possible further decompositions (for the 3 directions). A representation similar to Fig. 3 is obtained. For each value of λ , the cost function J is computed for each admissible R-D point. The decision of splitting or not the given subband is taken according to the minimum cost.

As an example, Fig. 3 shows a case for which the λ slope leads to take the decision of splitting the given subband in x direction.

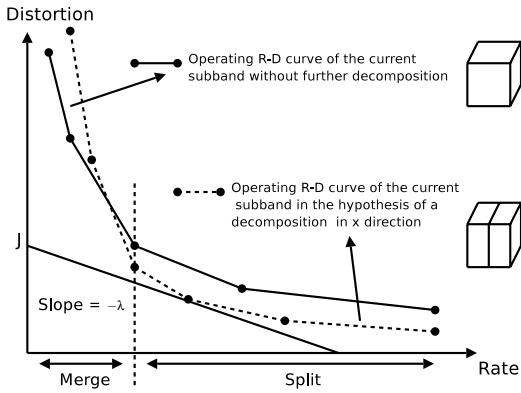


Fig. 3. Illustration of the split-merge decision during the algorithm. For clarity, R-D curves in the hypothesis of decomposition in the two other directions (y or spectral) are not represented and are considered to be above the others.

The search for the best basis is done as:

- Recursive function: $\text{cost}(W_{i,j,k}^{p,q,r}, \lambda)$
 - compute the cost $J_0 = J(\lambda)$ using Shoham and Gersho algorithm for the current subband
 - compute the cost J_1
 - if the minimum size is not reach for the rows: $J_1 = \text{cost}(W_{i+1,j,k}^{2p,q,r}, \lambda) + \text{cost}(W_{i+1,j,k}^{2p+1,q,r}, \lambda)$ by recursive calls.
 - otherwise $J_1 = \infty$
 - compute the cost J_2 : similar to J_1
 - compute the cost J_3 : similar to J_1
 - return the value $\min\{J_0, J_1, J_2, J_3\}$
- Global Function
 - For each λ : call $\text{cost}(W_{0,0,0}^{0,0,0}, \lambda)$

- Full rate-distortion curve for the given image

This algorithm leads to a different decomposition for each image and each targeted bitrate.

4. RESULTS

4.1. Context

The biorthogonal wavelet used in JPEG-2000 standard ((9,7) filter) is applied to the images. The distortion is measured based on squared error but to make comparison easier, the mean square error is converted to Peak Signal to Noise Ratio (PSNR) on the curves. The relation between PSNR and Mean Square Error (MSE) is defined by $PSNR = 10 \log_{10}((2^B - 1)^2 / MSE)$, B being the number of bits per sample. For hyperspectral images, the number of bits per digital value is 16, explaining the high values attained by the PSNR. For *Barbara* image, the original number of bits per pixel is 8.

The number of bits necessary to code the subband coefficients is evaluated using the arithmetic coder defined in [9].

4.2. On 2D images

The search for the best wavelet decomposition has been first applied to natural 2D images. For some images (the well-known *Lena* for example), the best wavelet decomposition is not so far from the classical multiresolution decomposition. However, in the case of images containing strong frequency features, such as *Barbara* for example (Fig. 4), the decomposition manages to concentrate the energy in very few subbands (subband 1) and manages to group many coefficients within the same subband (subband 2). The gain can reach 1.5 dB compared to the classical multiresolution decomposition as shown in Fig. 5.

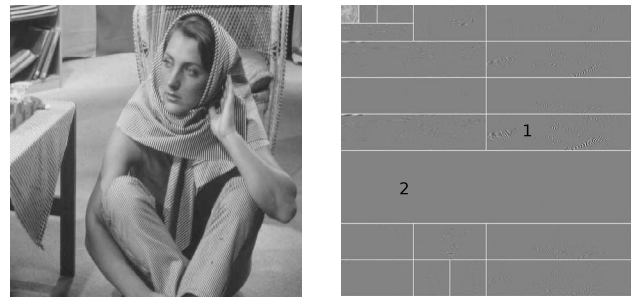


Fig. 4. Barbara image and the best anisotropic wavelet decomposition obtained for a bitrate of 0.9 bpp.

4.3. On hyperspectral images

The results obtained with the algorithm defined in 3.2 are compared with the algorithm used in Rosetta mission (ESA). The Rosetta algorithm was defined by Langevin [1] and is implemented on-board the Rosetta mission which

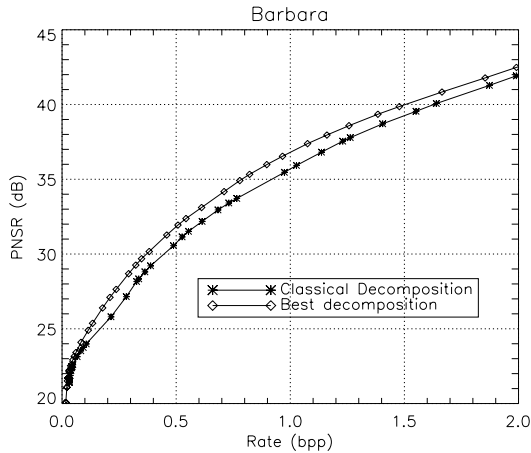


Fig. 5. Comparison between the classical decomposition and the best basis decomposition.

is currently travelling into space and will reach the comet 67P/Churyumov-Gerasimenko in 2014. This algorithm is based on an adaptation of SPIHT algorithm proposed by Said and Pearlman [10].

The results presented here are obtained on data from the AVIRIS hyperspectral sensor from JPL/NASA over the Moffett Field site in California (Fig. 1). Moreover, they were confirmed on different sites as well as on images acquired by the satellite sensor from NASA: Hyperion.

As can be seen from Fig. 6, the results of the isotropic decomposition are very close to the performances of the Rosetta algorithm. The best basis decomposition brings a clear improvement, leading to an increase of the quality of 8 dB. If the limit is fixed in term of quality, let say for example a PSNR greater than 70 dB, the necessary bit budget cuts down from 1 bit per pixel per band (bpppb) to 0.5 bpppb.

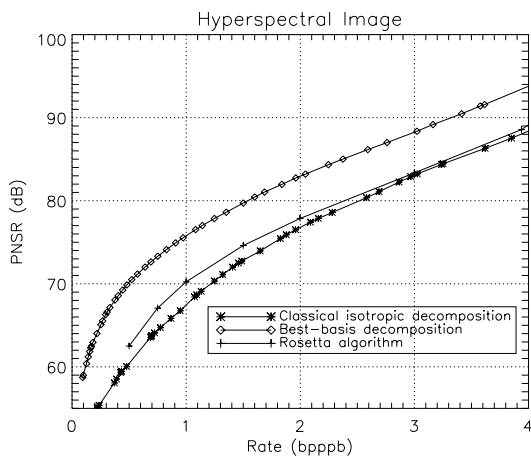


Fig. 6. Results on hyperspectral data, the anisotropic best-basis clearly improves the performances.

5. PERSPECTIVES

An adaptive wavelet transform was defined. On natural 2D images, the adaptative transform performs better than the usual transform but may not be sufficient to justify the increase in complexity. However, for hyperspectral images, the increase in performance is significant and enables a better use of the statistical properties of the data.

Therefore, it would be efficient to use the best decomposition to adapt compression principles such as SPIHT to define a compression system for hyperspectral images, especially if a particular fixed transform performs nearly like the adapting best decomposition.

6. ACKNOWLEDGEMENTS

This work has been carried out under the financial support of *Centre National d'Études Spatiales (CNES)*, *Office National d'Études et de Recherches Aéronautiques (ONERA)* and *Alcatel Space*. The authors wish to thank *NASA/JPL* for providing the hyperspectral images used during the experiments.

7. REFERENCES

- [1] Y. Langevin and O. Forni, "Image and spectral image compression for four experiments on the ROSETTA and Mars Express missions of ESA," in *Applications of Digital Image Processing XXIII* (SPIE, ed.), vol. 4115, pp. 364–373, SPIE, 2000.
- [2] X. Tang, W. A. Pearlman, and J. W. Modestino, "Hyperspectral image compression using three-dimensional wavelet coding," in *Image and Video Communications and Processing*, vol. 5022, pp. 1037–1047, SPIE, January 2003.
- [3] E. Christophe, D. Léger, and C. Mailhes, "Quality criteria benchmark for hyperspectral imagery," *IEEE Transactions on Geoscience and Remote Sensing*, vol. 43, pp. 2103–2114, September 2005.
- [4] K. Ramchandran and M. Vetterli, "Best wavelet packet bases in a rate-distortion sense," *IEEE Transactions on Image Processing*, vol. 2, pp. 160–175, April 1993.
- [5] D. Xu and M. N. Do, "Anisotropic 2D wavelet packets and rectangular tiling: theory and algorithms," in *Wavelets: Applications in Signal and Image Processing X.*, vol. 5207, pp. 619–630, SPIE, Nov 2003.
- [6] S. Mallat, "A theory for multiresolution signal decomposition: The wavelet representation," *IEEE Transactions on Pattern Analysis and Machine Intelligence*, vol. 11, pp. 674–693, July 1989.
- [7] "Optimal {3-D} Coefficient Tree Structure for {3-D} Wavelet Video Coding," *IEEE Transactions on Circuits and Systems for Video Technology*, vol. 13, no. 10, pp. 961–972, 2003.
- [8] Y. Shoham and A. Gersho, "Efficient bit allocation for an arbitrary set of quantizers," *IEEE Transactions on Acoustics, Speech, and Signal Processing*, vol. 36, pp. 1445–1453, September 1988.
- [9] A. Moffat, R. Neal, and I. H. Witten, "Arithmetic coding revisited," *ACM Transactions on Information Systems*, vol. 16, no. 3, pp. 256–294, 1998.
- [10] A. Said and W. A. Pearlman, "A new, fast, and efficient image codec based on set partitioning in hierarchical trees," *IEEE Transactions on Circuits and Systems for Video Technology*, vol. 6, pp. 243–250, June 1996.